

Simulation of the tubular positive electrode of the lead-acid battery

K. M. LIN, Y. Y. WANG, C. C. WAN

Department of Chemical Engineering, Tsing-Hua University, Hsin-Chu, Taiwan, ROC

Received 29 September 1987; revised 8 February 1988

The discharge performance of a tubular electrode of the lead-acid battery based on a pseudo steady-state approach was simulated. It was found that the discharge reaction started from the central interior region instead of from the outer surface as in the usual plate-type electrodes. This is due to the fact that the central region has a smaller reaction surface than the outer region of the tubular electrode. This consequently causes a higher current density near the center. A comparison of the theoretical prediction and experimental result shows that the model is fairly accurate except for very high rate discharge conditions.

1. Introduction

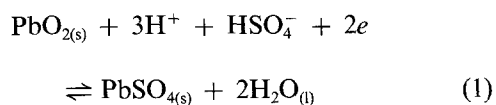
The application of computer simulation to a lead-acid plate-type battery system has been reported by several researchers. For example, Euler and Horn [1] investigated the current distribution in tubular electrodes by means of electrical analogues. Simonsson [2] developed a pseudo steady-state model which assumed a steady-state condition within each short time interval. He [3] also extended the model to the unsteady-state to accommodate large discharge current density conditions. Sunu [4] took into consideration the change of active material conductivity. Tiedemann and Newman [5] proposed a more generalized model in which the diffusion coefficient and conductivity are functions of temperature and concentration.

However, the simulation of another type of lead-acid battery, the tubular electrode, has been largely overlooked. In fact, the long life and dimensional stability of the tubular electrode, due to its outside tube shielding, have demonstrated its advantage and made the tubular-type lead-acid battery an important power source for industry.

The objective of this paper is to develop a model which can simulate the discharge performance of the tubular positive electrode of the lead-acid battery.

2. System simulation

The discharge behaviour of the tubular positive electrode can be described by the following equation:



The model is an extension of that developed by Simonsson [2] with the cylindrical coordinate system shown in Fig. 1 and the additional consideration of solid matrix conductivity.

The flux of H^+ and HSO_4^- can be expressed as the

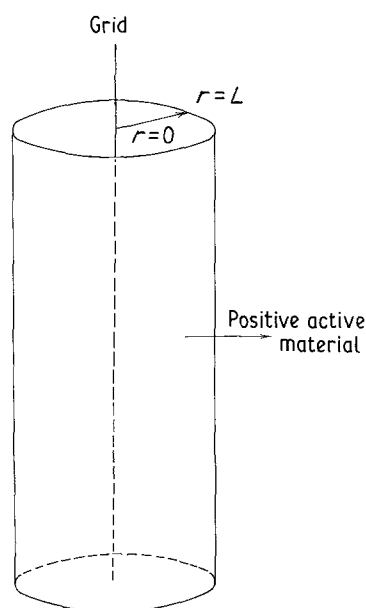


Fig. 1. Tubular positive electrode model.

sum of three terms due to diffusion, migration and convection, respectively.

$$J_i = -D_i \frac{\partial C_i}{\partial r} - C_i U_i \frac{Z_i}{|Z_i|} \frac{\partial \phi_2}{\partial r} + C_i v \quad (2)$$

where J_i is the flux of species i , D_i is the diffusion coefficient of species i , U_i is the ionic mobility of species i , Z_i is the charge of species i , ϕ_2 is the potential of the electrolyte and v is the electrolyte velocity. In addition, we denote H^+ by index 1 and HSO_4^- by index 2.

If the electroneutrality condition is obeyed, then

$$C_1 = C_2 = C \quad (3)$$

where C is the concentration of H_2SO_4 . We know that

$$i_2 = F \sum Z_i J_i = F(J_1 - J_2) \quad (4)$$

where i_2 is the current density in the electrolyte the electrolyte and F is the Faraday number. Substituting

Equations 2 and 3 into Equation 4 gives

$$i_2 = -k \frac{\partial \phi_2}{\partial r} - F(D_1 - D_2) \frac{\partial C}{\partial r} \quad (5)$$

where $k = F \Sigma Z_i / C_i U_i$, the effective conductivity of the electrolyte. Let

$$E = \phi_1 - \phi_2 \quad (6)$$

where E is the electrode potential and ϕ_1 is the potential of the solid matrix. Assuming that the solid matrix obeys Ohm's law, then

$$i_1 = -\sigma \frac{\partial \phi_1}{\partial r} \quad (7)$$

where i_1 is the current density of the solid matrix and σ is the effective conductivity of the solid matrix. Let

$$I = i_1 + i_2 \quad (8)$$

where I is the total current density, and substituting Equation 8 into Equation 7, we obtain

$$I - i_2 = -\sigma \frac{\partial \phi_1}{\partial r} \quad (9)$$

Solving Equations 5 and 9 together, we obtain

$$\left(\frac{1}{k} + \frac{1}{\sigma}\right) i_2 - \frac{I}{\sigma} = \frac{\partial E}{\partial r} - \frac{F}{k} (D_1 - D_2) \frac{\partial C}{\partial r} \quad (10)$$

Since

$$\eta = E - E_{\text{eq}}$$

where E_{eq} is the equilibrium potential and η is the overpotential, Equation 10 can be expressed as

$$\left(\frac{1}{k} + \frac{1}{\sigma}\right) i_2 - \frac{I}{\sigma} = \frac{\partial \eta}{\partial r} + \frac{\partial E_{\text{eq}}}{\partial C} \frac{\partial C}{\partial r} - (D_1 - D_2) \frac{F}{k} \frac{\partial C}{\partial r} \quad (11)$$

The kinetic expression for the electrode reaction is given by the following equation:

$$\frac{1}{r} \frac{\partial(r i_2)}{\partial r} = -S_0 \left(1 - \frac{X}{X_{\text{max}}}\right) i_0 \exp\left(-\frac{2F\eta}{RT}\right) \quad (12)$$

where S_0 is the initially available active surface in the fully charged electrode and i_0 is the exchange current density. Note that

$$X = -\frac{1}{q_0} \int_0^r \left[\frac{1}{r} \frac{\partial(r i_2)}{\partial r} \right] dt \quad (13)$$

where X is the degree of discharge, X_{max} is the maximum fraction of the electrode material that can be utilized at the actual current density and q_0 is the initially available quantity of charge per unit volume. The material balance for component 1 is

$$\frac{\partial(\varepsilon C_1)}{\partial t} = -\frac{1}{r} \frac{\partial(r J_1)}{\partial r} + N_1 \quad (14)$$

where ε is the porosity and N_1 is the source term for species 1. According to Simonsson's approach, we

also consider the structural change effect, so that

$$\varepsilon = \varepsilon_0 - g(1 - \varepsilon_0)X \quad (15)$$

where ε_0 is the initial porosity and g is a constant with a value of 0.917. Moreover

$$D_c = \frac{\varepsilon_0}{\varepsilon} D, \quad k_c = \frac{\varepsilon_0}{\varepsilon} k, \quad \sigma_c = \frac{\varepsilon_0}{\varepsilon} \sigma$$

where

$$D = \frac{2D_1 D_2}{D_1 + D_2}$$

Assuming the system is in the pseudo steady-state and the effect of convection is negligible, then Equation 14 can be rearranged to

$$\frac{3 - 2t_1}{2F} \frac{\partial(r i_2)}{r \partial r} + \frac{1}{r} \frac{\partial}{\partial r} \left(\frac{\varepsilon}{\varepsilon_0} D_c r \frac{\partial C}{\partial r} \right) = 0 \quad (16)$$

where t_1 is the transference number of species 1.

These equations can be transformed into the more convenient dimensionless forms as follows.

Let

$$\frac{i_2}{I} = i, \quad \frac{r}{L} = R', \quad \frac{C}{C_0} = C', \quad \eta' = \frac{F\eta}{RT}$$

$$E' = \frac{FE_{\text{eq}}}{RT}, \quad \tau = \frac{D_0 t}{L^2}$$

where L is the radius of tubular electrode, C_0 is the initial concentration of H_2SO_4 and D_0 is the diffusion coefficient at the initial condition. Consequently, Equations 11, 12, 13 and 16 become:

$$\left(\frac{D_c}{D_0}\right) \frac{\partial C'}{\partial R'} + (3 - 2t_1) \left(\frac{\varepsilon_0}{\varepsilon}\right) f i = 0 \quad (17)$$

where

$$f = \frac{IL}{2FD_0 C_0},$$

$$a \left(\frac{1}{\frac{k_0}{k_c} + \frac{k_0}{\sigma_c}} \right) \left(\frac{\varepsilon}{\varepsilon_0} \right) \frac{\partial \eta'}{\partial R'}$$

$$= \left[a \left(\frac{1}{\frac{k_0}{k_c} + \frac{k_0}{\sigma_c}} \right) \frac{\partial E'}{\partial C'} - b \left(\frac{\frac{k_0}{k_c}}{\frac{k_0}{k_c} + \frac{k_0}{\sigma_c}} \right) \right]$$

$$\times \left(\frac{D_0}{D_c} \right) (3 - 2t_1) f + 1 \left\} i - \left(\frac{\frac{k_0}{\sigma_c}}{\frac{k_0}{k_c} + \frac{k_0}{\sigma_c}} \right) \right.$$

(18)

where

$$a = \frac{k_0 RT}{FLI}, \quad b = \frac{F(D_1 - D_2)C_0}{IL}$$

and k_0 is the initial conductivity,

$$\frac{\partial i}{\partial R'} = h \left(1 - \frac{X}{X_{\max}} \right) \exp(-2\eta') - \frac{i}{R'} \quad (19)$$

where

$$h = -\frac{LS_0 i_0}{I}$$

and

$$X = -\frac{IL}{D_0 q_0} \int_0^{\tau} \frac{1}{R'} \frac{\partial(R'i)}{\partial R'} d\tau \quad (20)$$

The potential profile, concentration profile, reaction rate and the degree of discharge were calculated from Equations 17–20 by a Runge–Kutta method with the following two boundary conditions

$$R' = 0, \quad i = \frac{\partial C'}{\partial R'} = 0$$

$$R' = 1, \quad i = C' = 1$$

and the following initial condition

$$t = 0, \quad C' = 1, \quad X = 0$$

The numerical values of the parameters were the same in [3].

3. Results and discussion

3.1. Relationship between the electrode discharge characteristics and the discharge current density

Figure 2 shows that the electrode discharge charac-

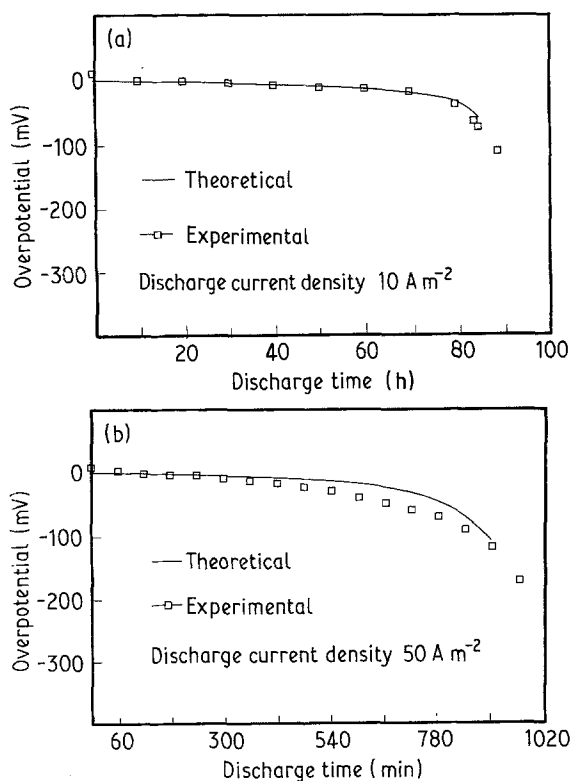


Fig. 2. Comparison between theoretical and experimental discharge curves. (a) Discharge current density = 10 A m⁻²; (b) discharge current density = 50 A m⁻².

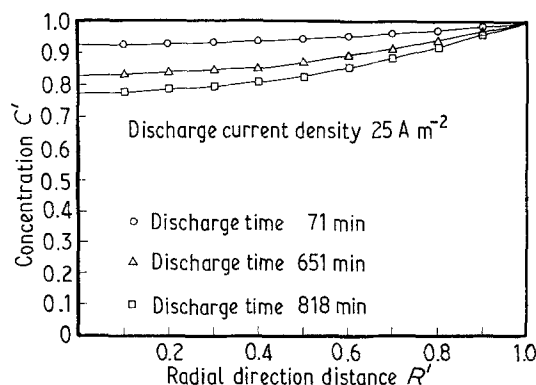


Fig. 3. The concentration distribution of tubular positive electrode with discharge current density = 25 A m⁻².

teristics obtained from the simulation agree well with the experimental results. However, as the current density increases, the discrepancy becomes more apparent. Furthermore, the deviation is larger in the final stage of discharge. This is mainly due to the assumption that the system is in the pseudo steady-state, which is not accurate for larger current density.

According to Peukert's relation [6], the relationship between the electrode capacity and the discharge current density can be described as follows:

$$t = \frac{K}{I^n} \quad (21)$$

where t is the discharge duration, I is the discharge current density and K and n are constants. From the results of Fig. 2, n can be calculated. n is approximately 1.3 and 1.1 for tubular electrode radii of 0.3 or 0.1 cm, respectively. Thus, the thicker the tubular electrode, the less efficient is the electrode utilization.

3.2. Distribution of H₂SO₄ concentration and reaction rate in the tubular electrode

Figure 3 shows that the concentration of H₂SO₄ decreases as the discharge proceeds and as the electrode radial direction decreases. This is due to the difficulty of replenishment of the consumed H₂SO₄ in the interior of the electrode. Comparing Figs 3, 4 and 5, we also observe that the consumption of H₂SO₄ increases as the discharge current density increases.

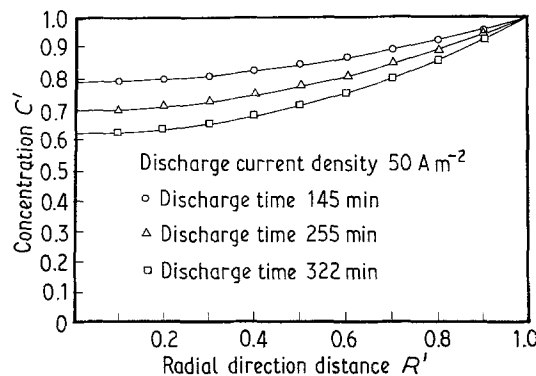


Fig. 4. The concentration distribution of tubular positive electrode with discharge current density = 50 A m⁻².

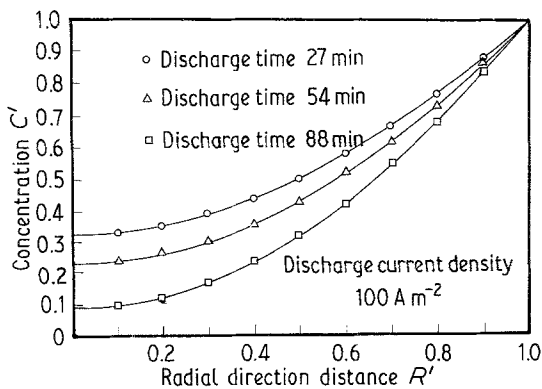


Fig. 5. The concentration distribution of tubular positive electrode with discharge current density = 100 A m^{-2} .

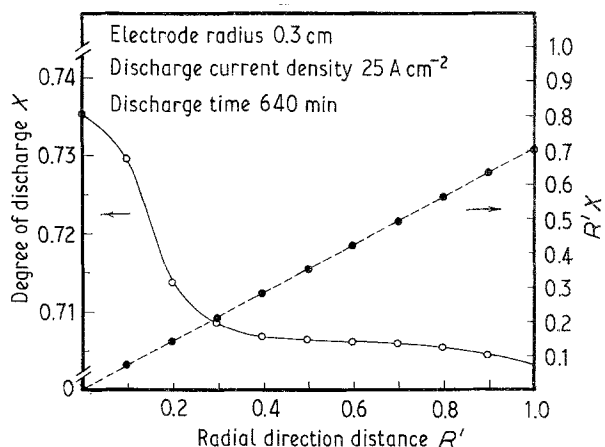


Fig. 8. Degree of discharge distribution of tubular positive electrode with electrode radius = 0.3 cm.

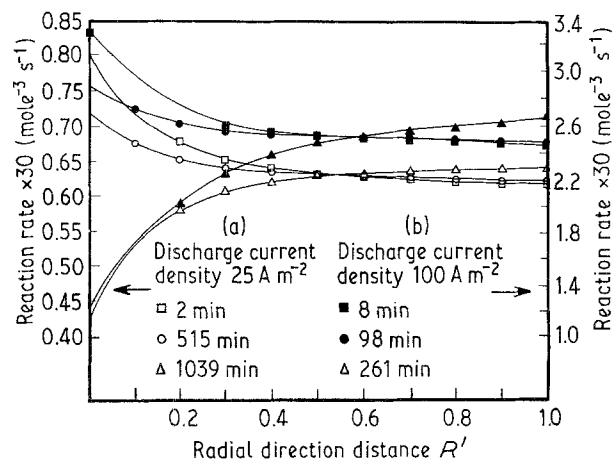


Fig. 6. The reaction rate distribution of tubular positive electrode. (a) Discharge current density = 25 A m^{-2} ; (b) discharge current density = 100 A m^{-2} .

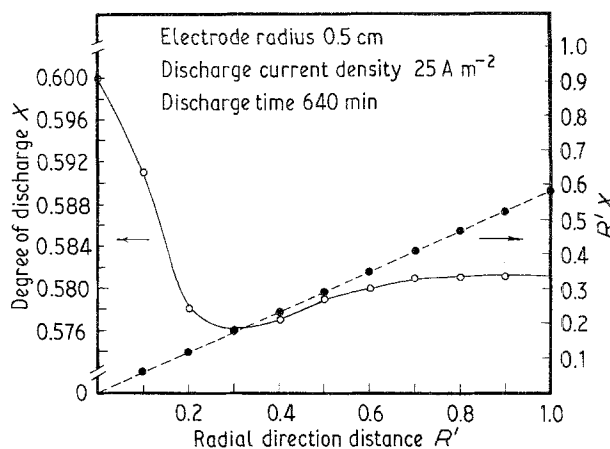


Fig. 9. Degree of discharge distribution of tubular positive electrode with electrode radius = 0.5 cm.

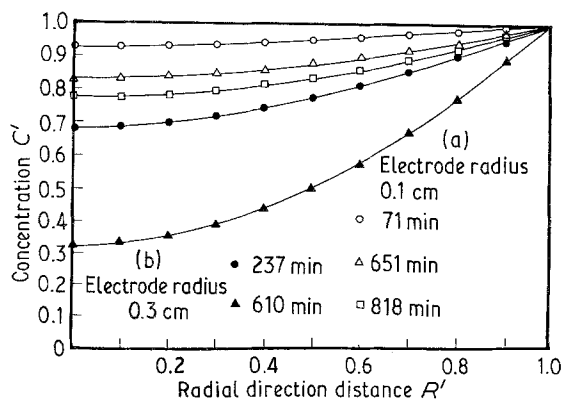


Fig. 7. The concentration distribution of tubular positive electrode. (a) Electrode radius = 0.1 cm; (b) electrode radius = 0.3 cm.

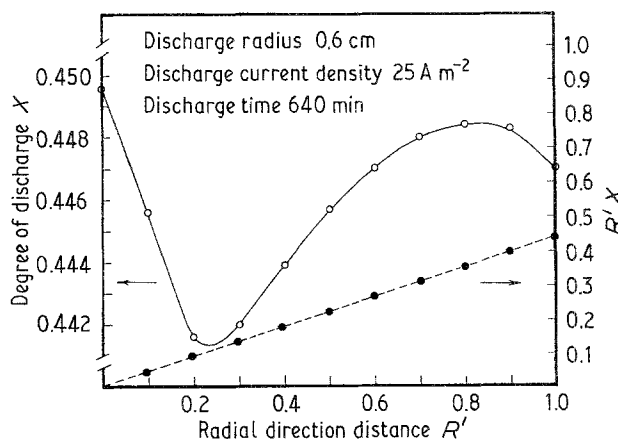


Fig. 10. Degree of discharge distribution of tubular positive electrode with electrode radius = 0.6 cm.

Figure 6 shows that, at the beginning of discharge, the reaction rate in the region near the collector is much higher than that outside the electrode. On the contrary, towards the end of discharging, the reaction rate in the interior of the electrode decreases significantly due to exhaustion of the reactants. This phenomenon is probably due to the geometrical structure of the tubular electrode which causes a higher current density in the interior of the electrode. Note that the discharging in plate-type electrodes generally starts from the exterior [3].

3.3. The effect of thickness of the tubular electrode

From Fig. 7 it is seen that the consumption of H_2SO_4 increases as the thickness of the tubular electrode increases. This means that the mass transfer is inefficient as the thickness of the tubular electrode increases. Consequently, it is more difficult to replenish the H_2SO_4 inside the electrode and the utilization of active material is lower.

Figure 8 shows that the degree of discharge is quite uniform when the radius of the tubular electrode is 0.3 cm. However, it becomes less uniform as the electrode thickness increases (Figs 9 and 10). It is worth noting that there is a minimum at about $R' = 0.2$. We believe that this is due to both the difficulty of transferring H_2SO_4 and the current density dropping in this region.

The dotted line in Figs 8–10 represents the relation between $R'X$ and R' . The total area below each curve

is directly proportional to the total effectiveness of active material in the electrode. It is obvious that the thickness of the electrode is inversely proportional to its effectiveness.

4. Conclusion

From the studies reported in this paper, we may make the following conclusions.

(i) At the beginning of discharge, the reaction rate in the interior of a tubular electrode is much higher despite the fact that it is difficult to replenish H_2SO_4 in the interior. Clearly the smaller area of the interior of the tubular electrode allows higher current density which dominates the reaction rate.

(ii) Increasing the thickness of the tubular electrode results in a non-uniform reaction distribution in the radial direction. The minimum appears at the region near the collector as a result both of the smaller current density and the lack of supply of H_2SO_4 .

References

- [1] J. Euler and L. Horn, *Electrochim. Acta* **10** (1965) 1057.
- [2] D. Simonsson, *J. Appl. Electrochem.* **3** (1973) 261.
- [3] D. Simonsson, *J. Appl. Electrochem.* **4** (1974) 109.
- [4] W. G. Sunu, in 'Electrochemical Cell Design' (edited by R. E. White), Plenum Press, New York (1983) p. 357.
- [5] W. Tiedemann and J. Newman, in 'Battery Design and Optimization' (edited by S. Gross), The Electrochemical Society Proceedings Series, Princeton, New Jersey (1979) p. 23.
- [6] W. Peukert, *Electrotech. Z.* **18** (1897) 287.